

## The Oxidation Behaviour of Niobium Containing $\gamma$ -TiAl Based Intermetallics in Air and Argon/Oxygen

Hubertus Nickel<sup>1,\*</sup>, Nanxi Zheng<sup>1</sup>, Andreas Elschner<sup>2</sup>, and Willem J. Quadackers<sup>1</sup>

<sup>1</sup> Research Centre Jülich GmbH, Institute for Materials in Energy Systems 1, D-52425 Jülich, Federal Republic of Germany

<sup>2</sup> Bayer AG, Krefeld, Federal Republic of Germany

**Abstract.** The oxidation behaviour of  $\gamma$ -TiAl based alloys with different Nb contents (2–10 At.%) was investigated in air and in argon-20% oxygen at 900 °C using thermogravimetric analysis. The oxide scales were characterized by a combination of optical microscopy, SEM/EDX and X-ray diffraction analyses. Although in all studied cases the presence of niobium improves the oxidation resistance of  $\gamma$ -TiAl, the oxidation kinetics, scale morphology and composition in air differed strongly from that in argon-oxygen. In air the oxidation resistance increases with increasing niobium-content. In Ar/O<sub>2</sub> the niobium dependence is far more complex because internal oxidation occurs which is favoured by the presence of niobium. SNMS analysis revealed that the differences in behaviour in the two atmospheres are related to the formation of Ti-rich nitride at the scale/alloy interface during air oxidation. The positive effect of niobium on the oxidation resistance of  $\gamma$ -TiAl is mainly caused by a decrease of the transport processes in the heterogeneous TiO<sub>2</sub>/Al<sub>2</sub>O<sub>3</sub>-surface scale. Nitride formation and/or niobium enrichment at the scale/alloy interface also affect the oxidation behaviour, however these factors are believed to be the result of the decreased transport processes rather than the main reason for the niobium effect.

**Key words:** oxidation, titanium aluminide, SNMS, niobium effect, oxygen tracer.

Due to the combination of low density with significant high temperature strength [1]  $\gamma$ -TiAl-based intermetallics are potentially suitable construction materials for a number of high temperature components such as blade materials in aero engines and industrial gas turbines. A major difficulty in respect to such applications is the poor oxidation resistance of titanium aluminides at temperatures above 700 °C [2, 3, 4]. Considerable effort has been devoted to the improvement of the oxidation behaviour of  $\gamma$ -TiAl-based intermetallics by addition of ternary and quaternary components. Addition of the element niobium significantly increases the oxidation

\* To whom correspondence should be addressed

resistance of TiAl [2, 4, 7], however the mechanisms have not been clarified. A complicating factor in the understanding of TiAl-oxidation is the fact, that the oxidation behaviour in air significantly differs from that in (argon-)oxygen. Whereas most authors find for binary titanium aluminides presence of nitrogen in the atmosphere to be detrimental for the oxidation resistance [8, 9], the opposite effect has also been observed [4]. Recently it has been shown, that for alloy Ti 48Al 5Nb, the oxidation resistance in air is better than in Ar/O<sub>2</sub> [9].

In the present study, the effect of niobium content (2–10A t.%) on the oxidation resistance of  $\gamma$ -titanium aluminide in air and Ar/O<sub>2</sub> was studied. To clarify the effect of nitrogen on the oxide growth mechanisms, scale analyses by light and electron microscopy were combined with SNMS depth profiling. The last mentioned method was also used for scale analysis after two-stage oxidation using <sup>18</sup>O<sub>2</sub>-tracer.

## Experimental

The following alloy compositions were produced by induction melting in an argon atmosphere (additions in At.-%): Ti 45Al, Ti 45Al 2Nb, Ti 45Al 5Nb, Ti 45 Al 10Nb, Ti 48 Al 5Nb. Disk specimens of 10 mm diameter and 2 mm thickness were prepared from the cast ingots and then ground to a 1200 grit surface finish. The oxidation kinetics at 900 °C in air and in argon + 20% oxygen were investigated using a ROBAL thermobalance.

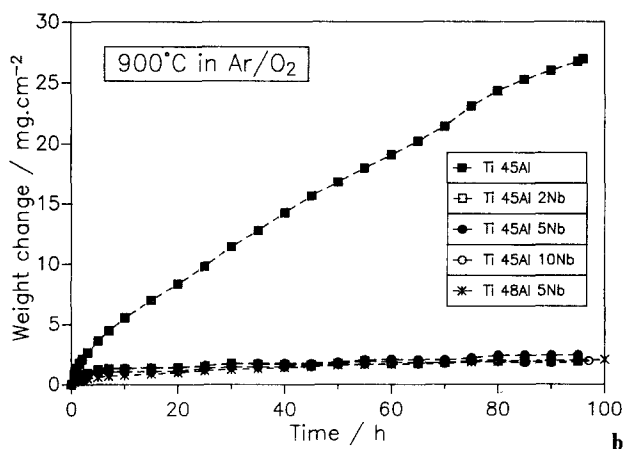
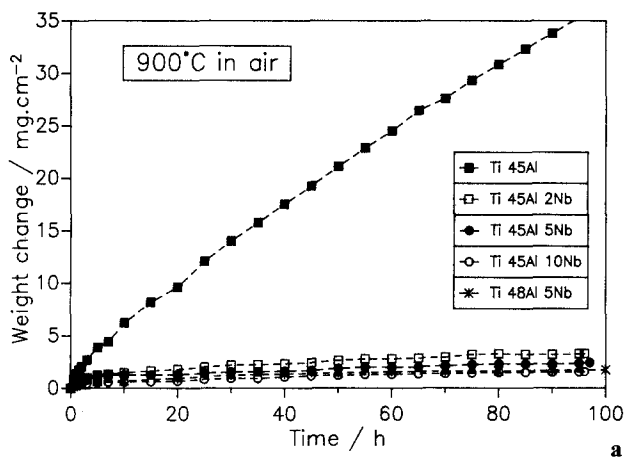


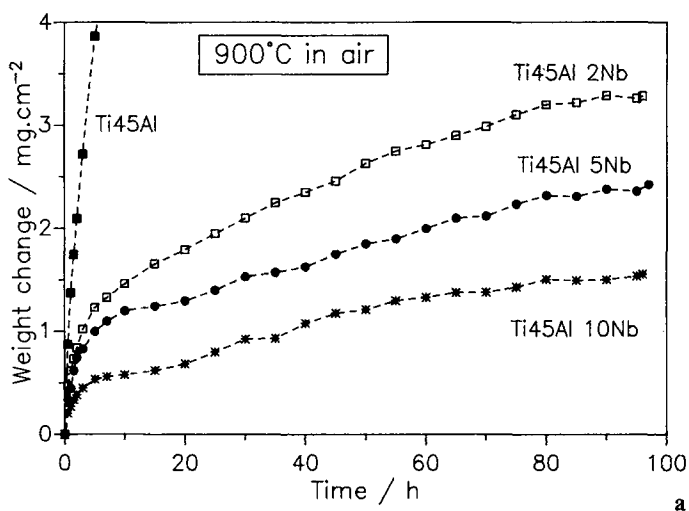
Fig. 1. Thermogravimetric analyses of the various alloys during oxidation in **a** air and **b** argon-oxygen at 900 °C

Specimens were examined before and after oxidation using optical microscopy, scanning electron microscopy (SEM), energy dispersive X-ray analysis (EDX) and X-ray diffraction (XRD). For studying oxide growth mechanisms, specimens of alloy Ti 48Al 5Nb were oxidized in a two-stage oxidation process [10, 11], using  $^{18}\text{O}_2$  in the second oxidation stage. The formed scales were analysed by secondary neutrals mass spectrometry (SNMS; INA3) [11].

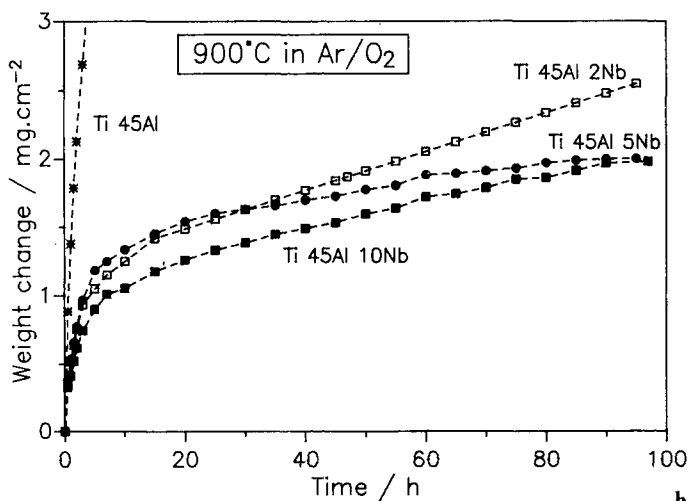
### Oxidation Behaviour

Figures 1 and 2 show mass changes as a function of time during isothermal oxidation of the various alloys at  $900^\circ\text{C}$  in air and in argon/oxygen. In both atmospheres all niobium containing materials show significantly lower oxidation rates than the binary alloy.

In air, the oxidation rate of the alloys with 45% Al decreases with increasing Nb-content (Fig. 2a). Light and electron optical analyses of metallographic cross sections show similar compositions of the oxide scales for all Nb-containing alloys (Fig. 3). SEM/EDX revealed, that the scales consist of an outer  $\text{TiO}_2$  layer beneath which an  $\text{Al}_2\text{O}_3$ -rich layer is present. The inner part of the scale consists of



a



b

**Fig. 2.** Enlarged view of the data in Fig. 1 for the alloys with 45%Al obtained during oxidation at  $900^\circ\text{C}$  in **a** air and **b** argon-oxygen

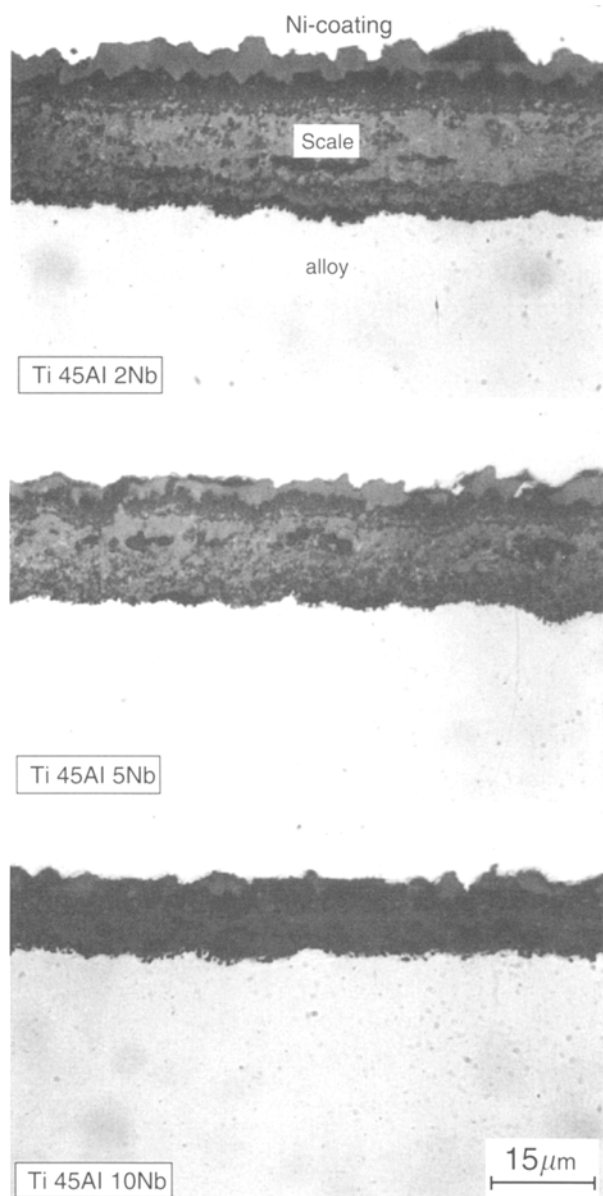


**Fig. 3.** Metallographic cross sections of the niobium containing alloys with 45%Al after 100 h oxidation at 900 °C in air

a  $\text{TiO}_2/\text{Al}_2\text{O}_3$ -mixture which is rich in aluminium near the scale/metal interface. This type of scale composition has extensively been described by several authors [4, 6, 7]. Careful analysis by optical microscopy sometimes revealed presence of a yellowish coloured layer with dark particles at the oxide/alloy interface. Based on SEM/EDX and XRD analyses, the yellowish coloured phase is titanium-rich nitride, however unequivocal determination of this nitrogen containing phase is extremely difficult with electron optical analysis techniques. In some cases the presence of  $\text{Ti}_2\text{AlN}$  next to  $\text{TiN}$  could be detected by XRD, although the unequivocal characterization of the thin nitride layer was not always possible because of the relatively thick oxide scale.

In Ar/O<sub>2</sub> no clear dependence of the oxidation rate for the alloys with 45% Al on the niobium content is detected (Fig. 2b). In the beginning of the oxidation a small dependence of oxidation rate on the Nb content might exist. After longer times however, the total oxygen uptake e.g. of the alloy with 2% Nb seems to become even smaller than that of the alloy with 10% Nb.

The metallographic cross sections confirm the results of the thermogravimetric analyses, i.e. also in Ar/O<sub>2</sub> all three niobium containing alloys formed oxide scales which are much thinner than that on Ti45Al (Fig. 4). The morphology of the surface scales is similar to that described above. However, the two alloys with the highest Nb content exhibit a more or less classical internal oxidation which is embedded in an Al-depleted layer containing  $\alpha_2$ -Ti<sub>3</sub>Al [9]. The internal oxidation is more significant for the alloy with the highest niobium content (Fig. 4). The alloy with 2% Nb seems to show a transient state between external scale formation and internal oxidation.

The described differences in behaviour between oxidation in argon-oxygen and air also found for a Nb-containing alloy with a higher aluminium content, Ti 48Al 5Nb (Fig. 5).

As the weight change curves indicate that the oxidation rate of the 10% Nb alloy in Ar/O<sub>2</sub> tends to be accelerated after longer times (Fig. 2b), specimens of the three niobium containing alloys with 45% Al were exposed in Ar/O<sub>2</sub> up to 300 h, however without continuous weight measurement. Figure 6 shows, that after such long oxidation times, indeed the alloy with the highest niobium content not only exhibits the most pronounced internal oxidation as after 100 h, but it now also forms a surface scale which is considerably thicker than those on the other two Nb-containing other alloys (Fig. 6). Figure 7 shows the weight change data of Fig. 2b extended with 300 h data, which were qualitatively derived from the metallographic cross-sections in Fig. 6. Due to the interactions between scale formation and internal oxidation, the rate of total oxygen uptake measured by thermogravimetry for the Nb-containing alloys is strongly time dependent.

### Scale Growth Mechanisms

For obtaining more detailed information on the scale growth mechanisms, two-stage oxidation experiments with subsequent SNMS analyses were carried out with alloy Ti 48Al 5Nb. As SNMS only allows depth profiling of scales which are not thicker than a few micrometer, the two-stage oxidation experiments were carried out at 800 °C, where scale growth rates are significantly smaller than at 900 °C.

Figure 8 shows SNMS depth profiles of alloy Ti 48Al 5Nb after two-stage oxidation in air/air + <sup>18</sup>O<sub>2</sub> and Ar + <sup>16</sup>O<sub>2</sub>/Ar + <sup>18</sup>O<sub>2</sub> for 10 min/20 min. It is apparent that in both atmospheres an alumina-rich scale is formed at the surface. Beneath that, a titanium-rich oxide is formed. After air exposure a titanium-rich nitride is found at the oxide/alloy interface (Fig. 8a). After short time oxidation in both atmospheres the <sup>18</sup>O shows an enrichment at the outer surface whereas the <sup>16</sup>O does not. This indicates that the scale grows by cation diffusion or oxygen lattice transport [10, 11]. Also, near the oxide/metal interface a slight <sup>18</sup>O-enrichment relative to <sup>16</sup>O is found, indicating the occurrence of oxygen short circuit diffusion [11].

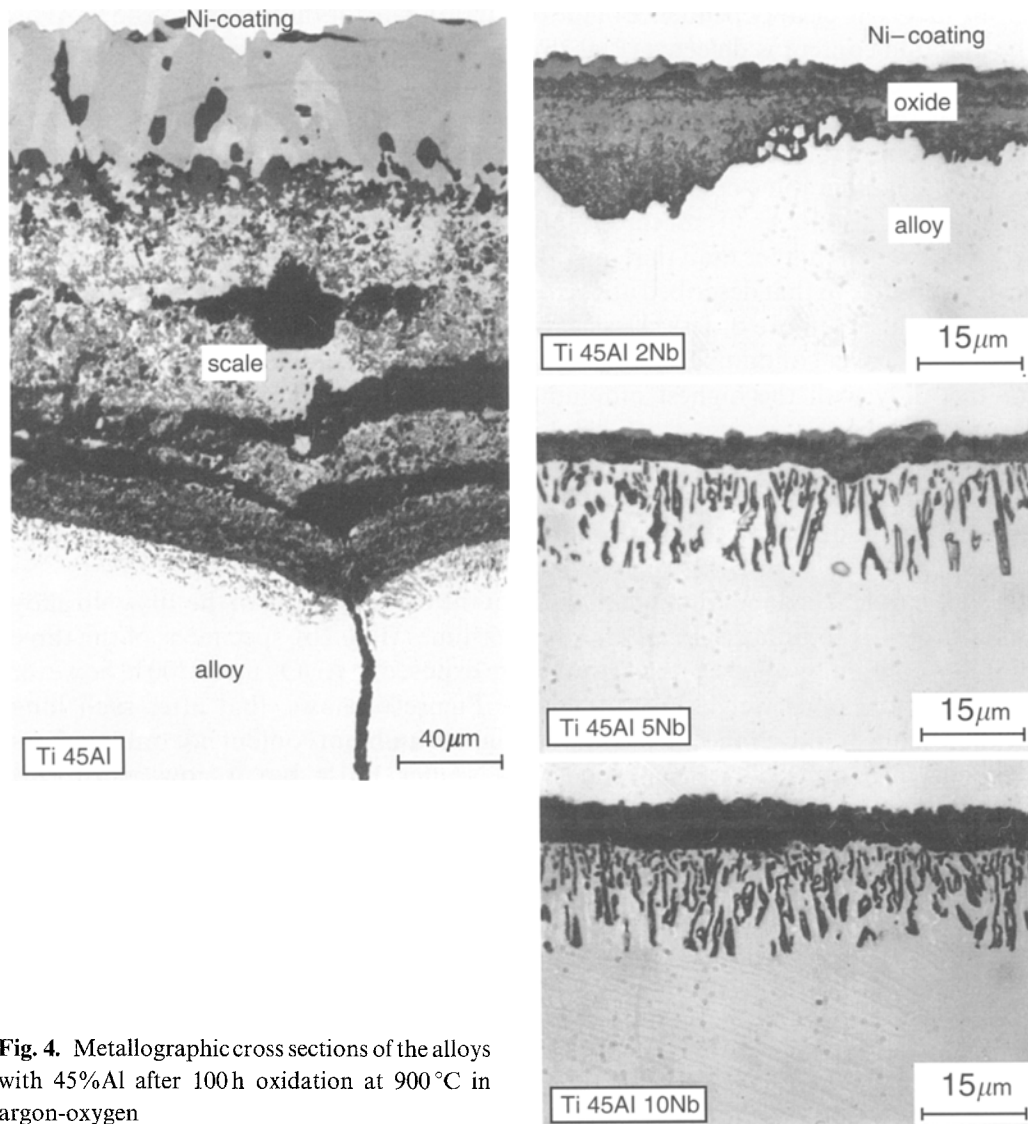


**Fig. 4.** Metallographic cross sections of the alloys with 45%Al after 100h oxidation at 900°C in argon-oxygen

After longer times (24 h/48 h) the  $^{18}\text{O}$  profile clearly shows two relative maxima (Fig. 9): one at the outer surface, indicating cation or oxygen lattice diffusion, and one in the inner part of the scale, revealing oxygen short circuit diffusion [11]. The initially formed alumina based layer (Fig. 8) is overgrown by titania (Fig. 9). This shows, that the outer  $^{18}\text{O}$  peak in Fig. 9 is at least partly related to outward titanium transport. It can presently not be deduced whether the short circuits along which the oxygen is transported inward are grain boundaries or e.g. microcracks. It is interesting to note that the maximum of the  $^{18}\text{O}$  in the inner scale is not located at the scale/alloy interface, but near the interface between the outer alumina-rich barrier layer [4] and the inner titania-rich layer (Fig. 9).

The following important differences between the profiles obtained after exposure of Ti 48Al 5Nb in air and Ar/O<sub>2</sub> are observed:

- during air exposure titanium-rich nitride is formed at the scale/alloy interface. Unlike the case for binary  $\gamma$ -titanium aluminide [12] the nitride sub-scale remains stable during long time oxidation.
- the separate layers titania/alumina/titania seem to be more “pure” after air exposure, whereas they seem to be more or less intermixed after exposure in Ar/O<sub>2</sub> (Fig. 9).
- an Al-depletion and an oxygen solubility in the sub-surface zone exist after Ar/O<sub>2</sub> exposure (Figs. 8 and 9); an Al-enrichment occurs in air (Fig. 9a).

### Discussion

The thermogravimetric and metallographic analyses have shown, that in argon/oxygen as well as in air, niobium additions between 2 and 10% significantly decrease the oxidation rates of  $\gamma$ -titanium aluminide. The dependence of the oxidation rate on the niobium content however strongly differs in air and argon-oxygen. Figure 10 shows the dependence of the oxidation rate constant  $K_p$  (defined as  $(\Delta m)^2 = K_p \cdot t$ , in which  $\Delta m$  is the specific weight change and  $t$  the oxidation time) for the three niobium containing alloys during oxidation in air. The results clearly show, that the oxidation resistance continuously increases with increasing niobium content. The oxidation rate dependence on Nb-content during exposure in Ar/O<sub>2</sub> is far more complex (Fig. 11). This is caused by the fact, that in argon-oxygen not only scale formation but also internal oxidation embedded in an oxygen containing depletion layer occurs (Figs. 4 and 5). The extend of the internal oxidation increases with increasing Nb content (Fig. 6).

The present investigations clearly show that the oxidation mechanisms during air exposure of niobium containing  $\gamma$ -TiAl cannot be explained solely by classical thermodynamic and kinetic aspects of alloy oxidation because during air exposure presence of nitrogen plays a significant role: formation of titanium-rich nitride was found at the scale/alloy interface after short as well as long time oxidation.

In the early stages of oxidation the oxide scales formed in air do, apart from the nitride layer at the scale/alloy interface, not significantly differ from those formed in argon-oxygen: in both cases an alumina-rich scale is formed at the surface (Fig. 8). After longer times this scale becomes in both atmospheres overgrown by titania (Fig. 9).

In the sub-surface layer formed on the niobium containing alloys in argon/oxygen, a depletion of aluminium and a dissolution of oxygen occurs. This depletion layer, which mainly consists of oxygen containing  $\alpha_2$ -Ti<sub>3</sub>Al [9], can also be seen in the metallographic cross sections in Fig. 5. It is however not observed after air oxidation (Figs. 3 and 5). The initial formation of an Al-depleted layer in argon/oxygen can be explained by the fact that, in spite of the heterogeneous scales which are being formed, alumina rather than titania must be considered to be the thermodynamically stable oxide on  $\gamma$ -TiAl based intermetallics [4, 13]. However, due to the high oxygen solubility of the sub-surface layer, the aluminium tends after

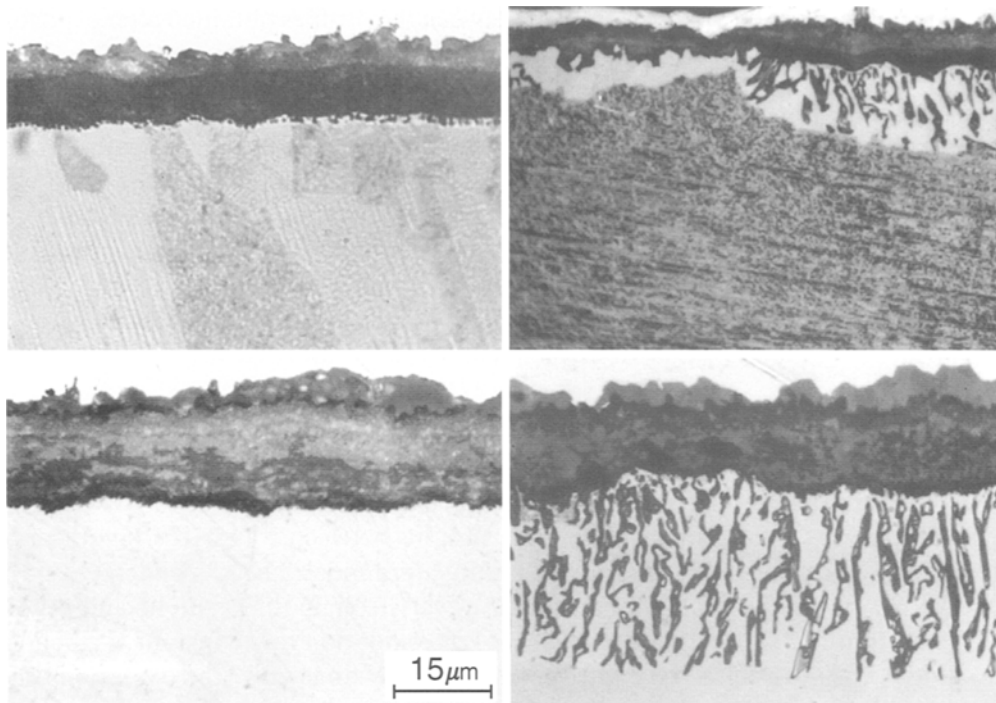


**Fig. 5.** Metallographic cross sections of Ti 48Al 5Nb after 100 h (upper) and 300 h (lower) oxidation in argon-oxygen (right) and air (left) at 900 °C

longer oxidation times to become oxidized internally rather than forming a protective external scale.

Considering the classical conditions for the transition from scale formation to internal oxidation [14], the niobium concentration dependence for the occurrence of internal oxidation (Figs. 4 and 6), could be caused by the fact that niobium increases the oxygen solubility and/or diffusivity in the sub-surface layer; it also could decrease the aluminium solubility and/or diffusivity. Because of the limited information available concerning the ternary and quaternary phase diagrams of Ti, Al, Nb, O it can presently not be derived with certainty which of the mentioned factors is dominating.

An interesting observation is, that in Ar/O<sub>2</sub> the alloy with the highest niobium content, which initially seems to possess the best oxidation resistance (Fig. 2b), after longer times not only shows the most pronounced internal oxidation (Fig. 4), but eventually also the highest scale growth rate (Fig. 6). This is caused by the fact that the aluminium becomes tied-up in the internal oxidation zone. Consequently it can not diffuse into the surface scale which therefore becomes very rich in titanium leading to accelerated oxide growth rates after longer oxidation times (Fig. 6).

Due to the strong dependence of the oxidation mechanisms of niobium containing  $\gamma$ -titanium aluminides in argon-oxygen on time and exact alloy composition, results of experiments carried out in various laboratories are difficult to compare. Figure 11 qualitatively shows the contribution of scale growth and internal oxidation to the total oxygen uptake (i.e. weight change detected by thermogravimetric



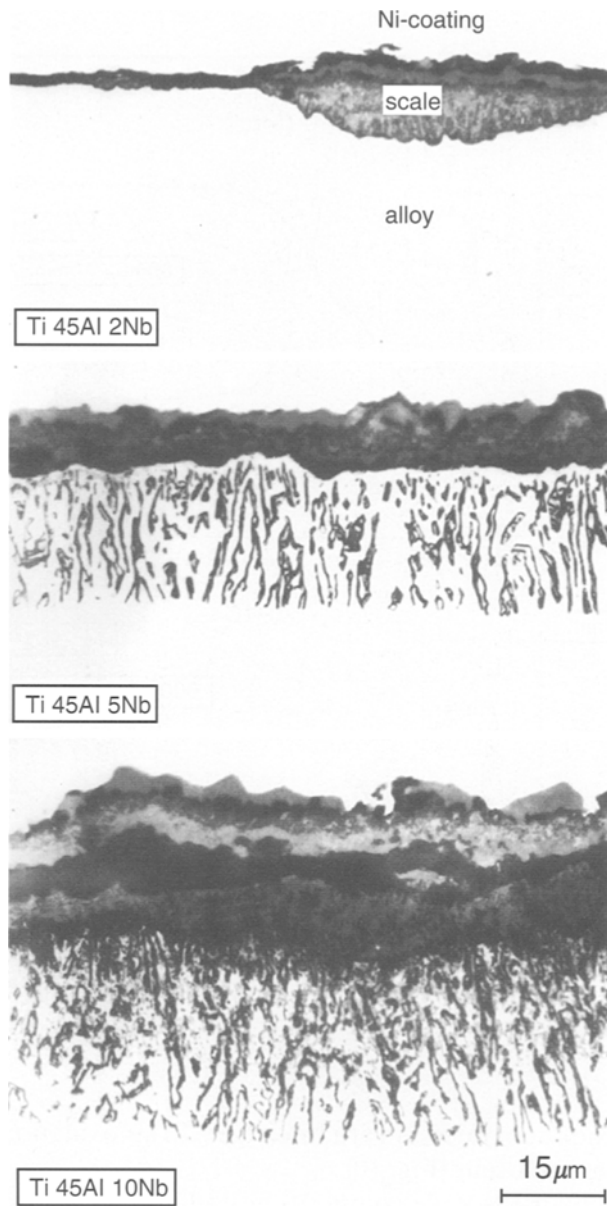


**Fig. 6.** Metallographic cross sections of the niobium containing alloys with 45%Al after 300 h oxidation at 900 °C in argon-oxygen

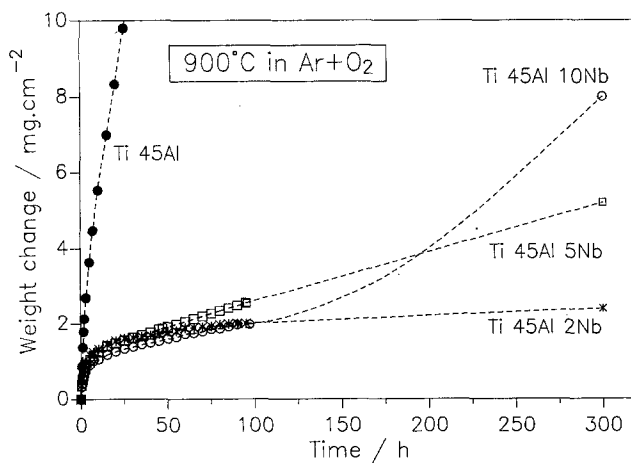


**Fig. 7.** Weight change data from figure 2b (Ar/O<sub>2</sub>, 900°) extended with 300 h data approximated from the metallographic cross sections in Fig. 6

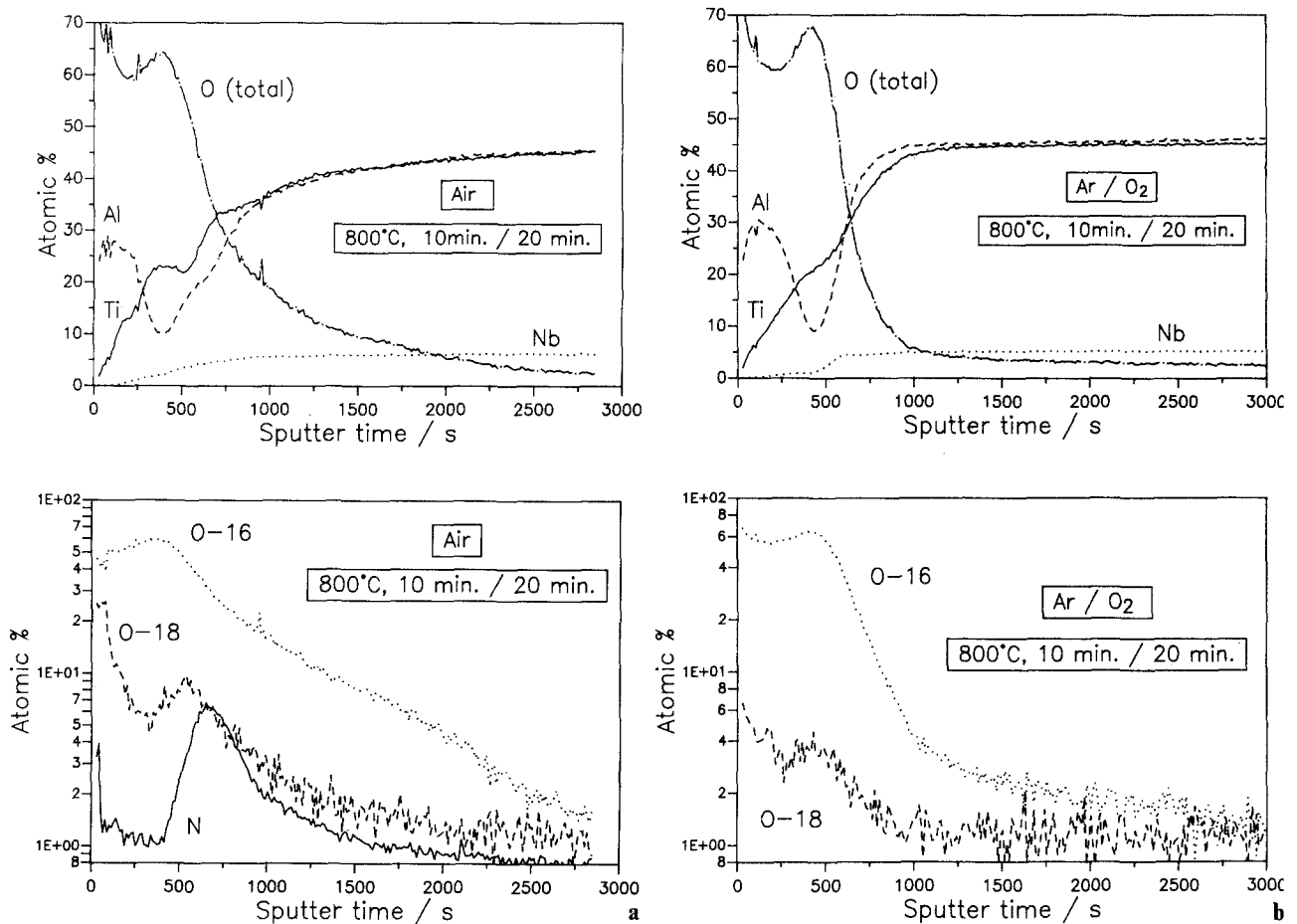


**Fig. 8.** SNMS analyses of surface scales on Ti 48Al 5Nb formed during two-stage oxidation (10 min/20 min) at 800 °C in **a** air/air +  $^{18}\text{O}_2$  and **b** Ar- $^{16}\text{O}_2$ /Ar- $^{18}\text{O}_2$

analysis) at various stages of the oxidation process in argon-oxygen. In air oxidation this complex time dependence does not occur (Fig. 10).

As already mentioned above, in air the scale composition itself is in the early stages of oxidation not very different from that in argon-oxygen (Fig. 8). After longer times, however, the oxidation behaviour in the two atmospheres differs considerably. This difference is caused by the fact that in air an Al-depleted, oxygen-containing sub-surface layer is not being formed. The missing of this depletion layer is related to the presence of titanium-rich nitride at the oxide-metal interface (Figs. 8 and 9). Although also during air oxidation aluminium is clearly consumed from the alloy by scale formation, the formation of the nitride causes titanium to be consumed at an at least similar rate. The SNMS studies in Fig. 9, confirmed by the 100 h results in Fig. 12, show that in air even an aluminium enrichment rather than a depletion occurs in the sub-surface zone.

X-ray diffraction analyses of a number of specimens after air oxidation revealed that the nitride layer at the alloy/oxide interface consisted of the presence of TiN; sometimes additionally  $\text{Ti}_2\text{AlN}$  was found. If a continuous layer would be present,

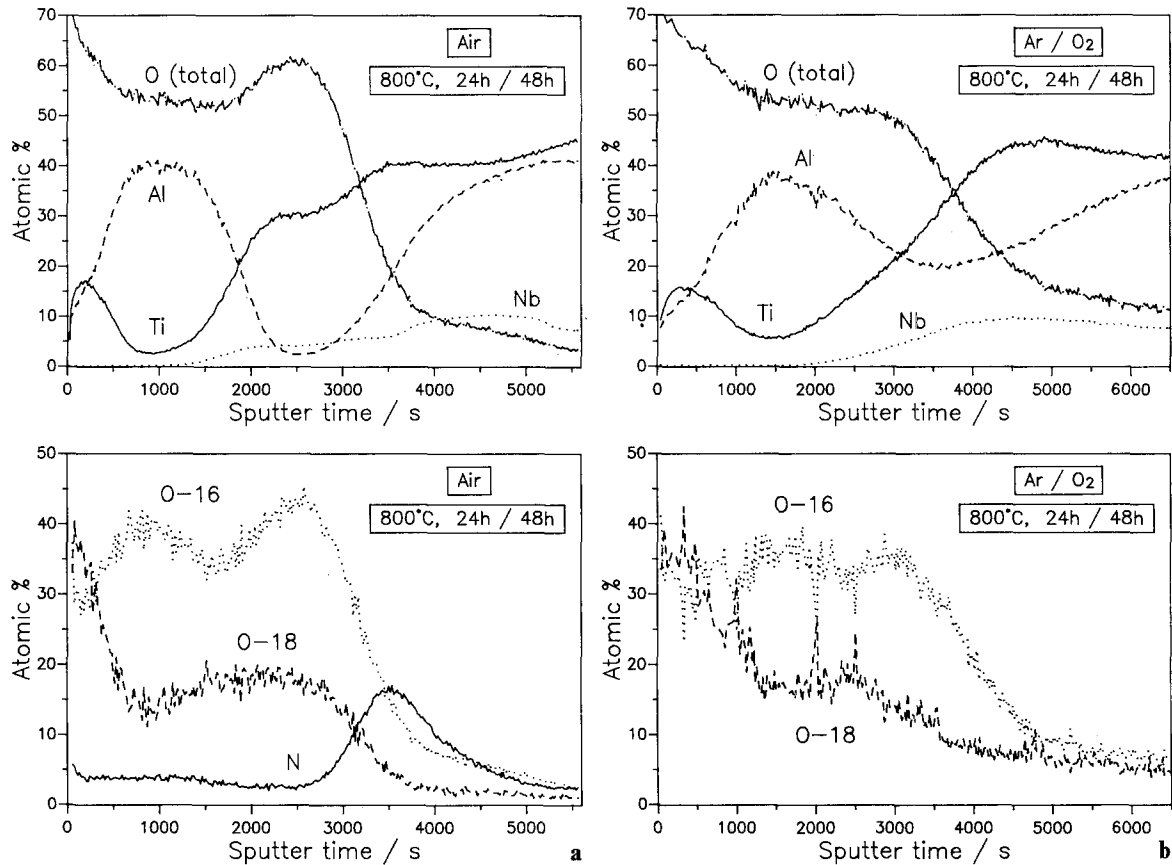
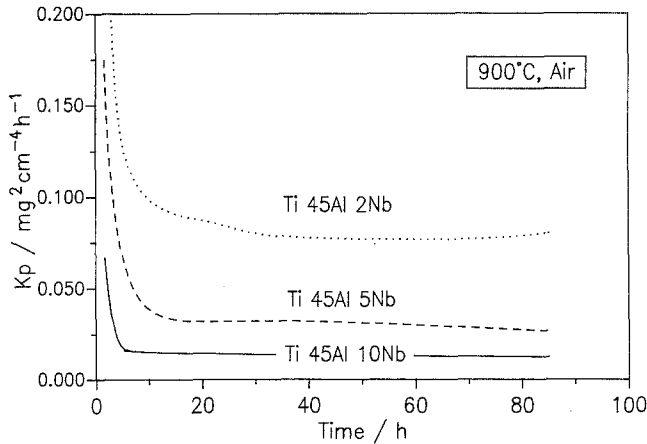


Fig. 9. Like Fig. 8 for 24h/48h

the nitrogen content measured by SNMS depth profiling should be 25–50 At %, i.e. much higher than actually measured (Figs. 8, 9, 12). It should, however, be mentioned that, if the thickness of the nitride layer is smaller than the “roughness” of the scale/alloy interface, the nitrogen signal during depth profiling will be “dispersed” leading to a measured maximum nitrogen content which is much smaller than that which is actually present in the nitride layer. Considering the significant roughness of the scale/alloy interface (Fig. 3) in combination with the numerous results of the metallographic analyses, in which a yellowish coloured layer was observed at the oxide/alloy interface, it is very likely that the nitride layer is indeed quite continuous. An interesting observation is, that the oxygen profile after 72 h oxidation shows a clear “kink” in the vicinity of the nitride layer (Fig. 9). This is caused by the small aluminium-rich oxide particles which are sometimes observed in the nitride layer at the nitride/alloy interface (Figs. 3 and 5) (see also ref. [4]).

The formation of a titanium-rich nitride layer has also been observed in the early stages of air oxidation of niobium-free binary titanium aluminides [12, 15, 16]. After already slightly prolonged oxidation however, this continuous nitride layer vanishes, probably due to transformation into oxide [12]. One might speculate, that the



**Fig. 10.** Time dependence of  $K_p$  for the niobium containing alloys with 45%Al during oxidation in air at 900°C. Data were derived from weight change results in Fig. 2a

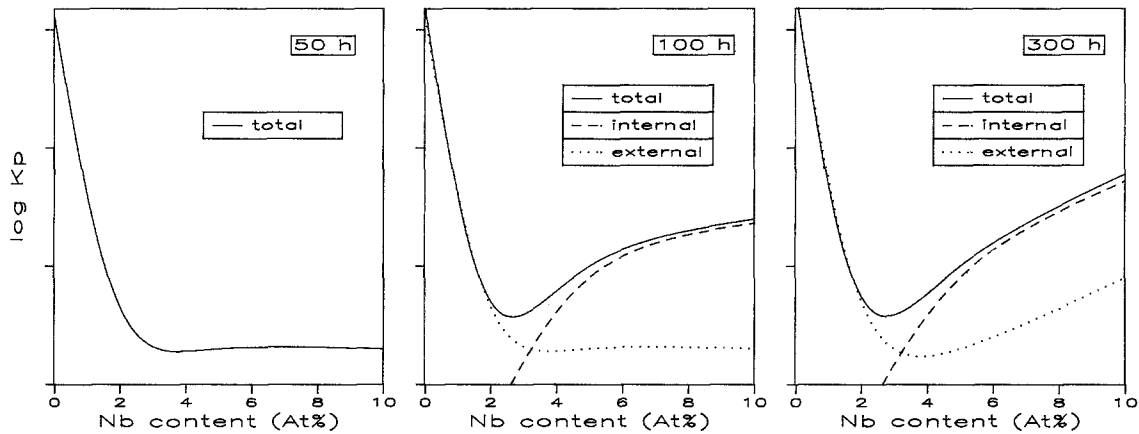


**Fig. 11.** Qualitative effect of niobium on  $K_p$ -values of alloys with 45%Al after different oxidation times in argon-oxygen. The data were approximated from weight change data and metallographic cross sections (Fig. 2b, 4, 6)

beneficial effect of niobium on the oxidation resistance is correlated with the long time stability of the nitride sub-surface layer (Figs. 9 and 12) which could act as a barrier against oxygen and/or metal diffusion. The present results however, clearly show, that this cannot be the main mechanism: although in a nitrogen-free atmosphere the oxidation critically depends on the exact niobium content due to occurrence of internal oxidation, the oxidation rates are also in argon-oxygen always much smaller than those of the niobium-free binary titanium aluminide (Fig. 4).

Niobium is found to be incorporated in the inner titania-rich part of the surface oxide and it becomes slightly enriched at the alloy/scale interface (Figs. 9 and 12). It is possible that this enrichment affects the diffusion processes in the sub-surface layer in a positive way. One would in that case however expect, that the beneficial effect of niobium should become only active after longer oxidation times, i.e. after a significant niobium-enrichment has occurred. This time delay has however not experimentally been observed: already in the very early stages of oxidation, the positive effect of niobium is being found.

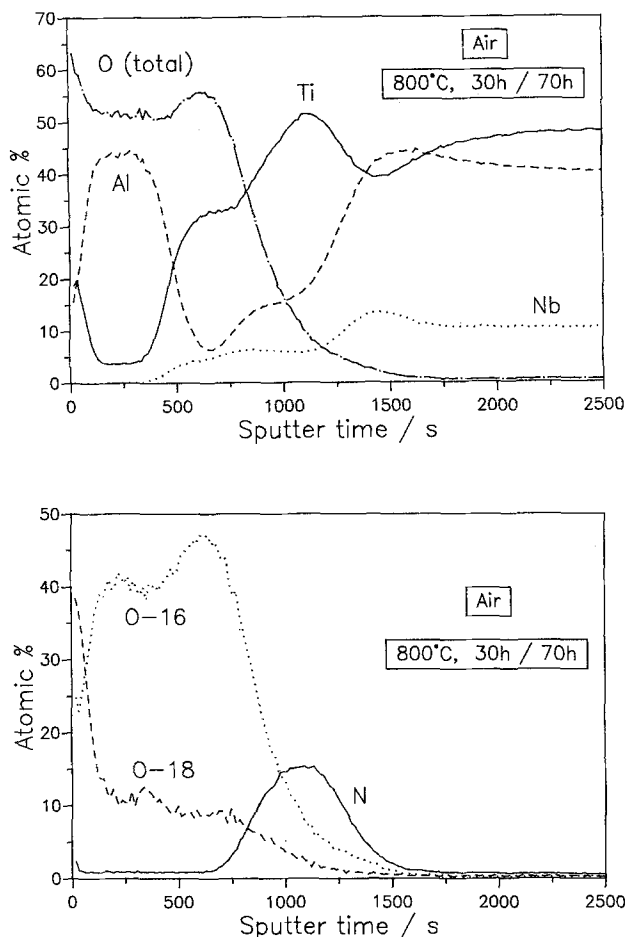


**Fig. 12.** SNMS depth profiles of surface scale on Ti 48Al 5Nb formed during two-stage oxidation (300 h/70 h) in air/air +  $^{18}\text{O}_2$  at 800 °C

Apart from that, the composition of the sub-surface depletion layer formed during argon-oxygen exposure of the Nb-containing alloys does, before the internal oxidation occurs, not significantly differ from that formed in binary  $\gamma$ -titanium aluminide. In all studied alloys it consists of  $\alpha_2$ -Ti<sub>3</sub>Al and a second phase, which is probably a ternary cubic Ti/Al/O-compound (lattice parameter 6.91 Å [9]). Apparently the niobium enrichment in this oxidation period is not sufficiently high for new, niobium containing ternary phases to be stabilized. A significant effect of the niobium enrichment on the diffusion processes in the sub-surface layer therefore seems to be unlikely.

Another observation which strongly indicates that the Nb-effect is not related to sub-surface nitride formation or niobium-enrichment is the fact that the beneficial effect of niobium addition is not only observed for titanium aluminide but also for pure titanium (Fig. 14). All these results therefore indicate, that niobium directly affects the transport processes in the heterogeneous alumina/titania-rich scale. If this scale on the titanium aluminide grows by lattice diffusion, a substitutional dissolution of Nb<sup>5+</sup> in the titania lattice would be expected to decrease the concentration of oxygen vacancies and titanium interstitials [17, 18], i.e. both the

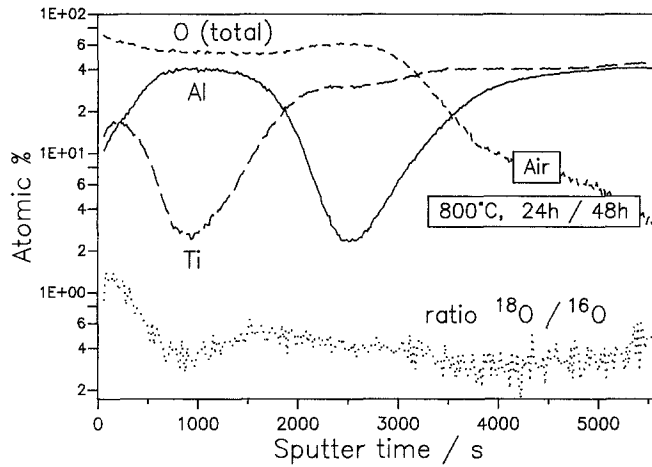


**Fig. 13.**  $^{18}\text{O}/^{16}\text{O}$ -ratio derived from the isotope profiles in Fig. 9a

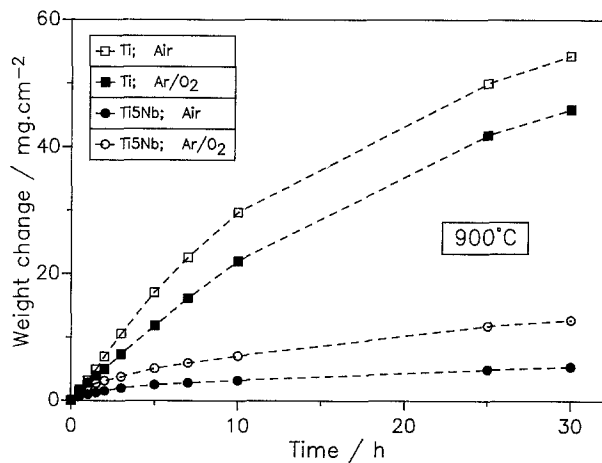
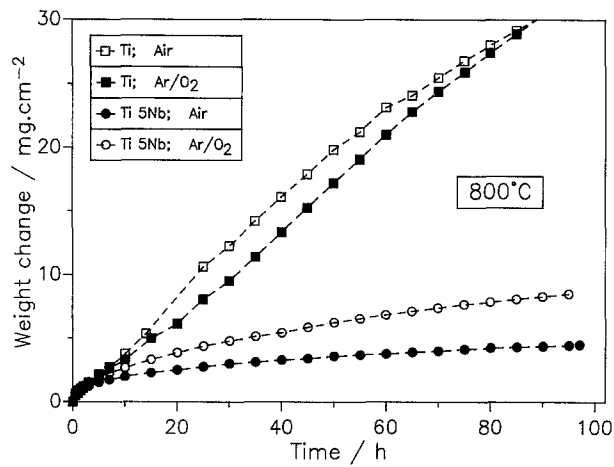


**Fig. 14.** Weight change data of Ti and Ti 5Nb at 800 and 900°C in air and argon-oxygen

oxygen inward and titanium outward transport would be decreased, in agreement with the experimental observations [4].

Assuming such a doping mechanism to prevail, the behaviour of binary and ternary, niobium containing  $\gamma$ -titanium aluminide in air and argon-oxygen can be explained in the following way:

- In argon-oxygen an alumina rich surface scale is formed in the early stages of oxidation. In the aluminium depleted sub-surface zone, initially a ternary Ti-Al-O compound is present [9]. After increased Al-depletion, additionally  $\alpha_2$ , which possesses a high oxygen solubility [9, 13], appears in the sub-surface layer. On further exposure the presence of oxygen containing  $\alpha_2$  causes the initial alumina layer to be changed to a mixed titania/alumina scale. This is accompanied by internal oxidation of aluminium to occur in the binary  $\gamma$ -TiAl as well as in the ternary Nb-containing alloys. For the binary alloy however, the growth rate of the heterogeneous alumina/titania scale is so high that the internal oxidation only insignificantly contributes to the overall oxygen uptake. The growth rate of the heterogeneous scale is decreased by niobium addition due to the above mentioned Nb-doping of the rutile.
- During air exposure both binary  $\gamma$ -TiAl and ternary Nb containing  $\gamma$ -TiAl initially form titania-rich nitride next to alumina. After transition to a mixed titania/alumina layer [4, 12, 15] presence of the nitride at the oxide/alloy interface prevents Al-depletion in the sub-surface layer. As the heterogeneous scale on the niobium-free alloy grows quite rapidly, the oxygen partial pressure at the scale/alloy interface eventually becomes sufficiently high for the titanium-rich nitride to become unstable relative to titanium oxide. Consequently the nitride vanishes after longer times and this is accompanied by formation of an Al-depleted sub-surface layer. In the niobium containing alloys, the growth of the mixed titania/alumina scale, and consequently the ingress of oxygen is significantly decreased by the above mentioned doping mechanism. By this fact, the oxygen partial pressure at the scale-alloy interface remains sufficiently low for the titanium-rich nitride to remain stable. The alloy immediately adjacent to this layer will therefore be depleted in titanium. As a consequence a relative Al-enrichment rather than Al-depletion occurs in the sub-surface zone. This effect facilitates the formation of a very thin alumina based oxide in the inner part of the heterogeneous scale adjacent to the alloy, which has also been described by other authors [4].

In this consideration, the effect of niobium addition in  $\gamma$ -TiAl on the stability of the nitride subscale during air oxidation is a result of the reduced oxygen transport in the heterogeneous titania/alumina scale rather than being the actual reason for the improved oxidation resistance.

The assumed reduction of oxygen transport in the heterogeneous scale by niobium is based on a classical doping theory in which the  $\text{Ti}^{4+}$  in the rutile lattice is replaced by  $\text{Nb}^{5+}$  ions. The  $^{18}\text{O}$ -enrichment after two-stage oxidation in the inner part of the scale (Figs. 9 and 12) however shows that the oxygen transport occurs via rapid diffusion paths. The ratio  $^{18}\text{O}/^{16}\text{O}$  (Fig. 13) indicates that the scale does not solely grow at the oxide/alloy interface but in the whole inner scale part, especially at the boundary between the inner titania-rich layer and the reprecipitated alumina-rich scale [16] which is located beneath the outer titanium oxide. It is presently not understood whether Nb reduces the oxygen rapid diffusion paths transport by acting as a “dopant” e.g. at the oxide grain boundaries in a similar way as described above for lattice diffusion or whether it behaves as a grain boundary segregant as described for yttrium in alumina based surface scales on NiCrAl- and FeCrAl-based alloys [19, 20, 21].

## Conclusions

Niobium additions between 2 and 10 At.% significantly improve the oxidation resistance of  $\gamma$ -TiAl based intermetallics in argon-oxygen and in air. Whereas in air the oxidation resistance increases with increasing niobium content, the optimum niobium addition during exposure in Ar/O<sub>2</sub> depends on oxidation time and probably temperature. The positive effect of niobium in both mentioned atmospheres is related to a direct decrease of the metal and oxygen diffusion in the heterogeneous alumina/titania surface scale. Due to the reduced oxygen transport compared to that in scales on niobium-free  $\gamma$ -TiAl, the nitride sub-layer which is initially formed during air exposure, remains stable after long oxidation times. This causes aluminium beneath the heterogeneous alumina/titania scale to become enriched in the alloy adjacent to the nitride layer, thereby facilitating the formation of very thin alumina scale in the inner oxide layer.

During argon-oxygen exposure of niobium containing  $\gamma$ -TiAl, the sub-surface layer beneath the heterogeneous Al<sub>2</sub>O<sub>3</sub>/TiO<sub>2</sub> scale becomes depleted rather than enriched in aluminium. Due to the high oxygen solubility of this layer, which consists of  $\alpha_2$  and a ternary Ti-Al-O compound, internal oxidation of aluminium occurs. This reduces the incorporation of aluminium into the scale leading to an accelerated scale growth after longer times. The tendency of aluminium to oxidize internally during Ar/O<sub>2</sub> exposure increases with increasing niobium content.

*Acknowledgements.* Thanks are due to the Deutsche Forschungsgemeinschaft (Bonn, FRG) which financially supported this investigation. The authors gratefully acknowledge Mr. Beys from KFA-SI and Mr. Lorenz from Research Centre GKSS (Geesthacht, FRG) for alloy manufacturing, Mr. Baumanns, Mr. Hoven, Mr. Lersch and Dr. Wallura From KFA/IWE are acknowledged for their assistance in carrying out the oxidation experiments, optical metallography, XRD and SEM/EDX.

## References

- [1] M. Yamaguchi, in: *Proceedings High Temperature Intermetallics, London, 30 April–1 May 1991*, The Royal Society, p. 15.
- [2] A. K. Misra, *Metal. Trans.* **1991**, 22A, 715.
- [3] M. Khobaib, F. Vahldiek, *2nd Int. SAMPE Metals Conference, Dayton, Ohio, Society for the Advancement of Materials and Process Eng., August 2–4, 1988*, Proc. p. 262.
- [4] S. Becker, A. Rahmel, M. Schorr, M. Schütze, *Oxid. Met.*, **1992**, 38, 425.
- [5] S. M. L. Sastry, H. A. Lipsitt, O. Izumi, H. Kimura, in: *Proc. 4th Int. Conf. Titanium Kyoto 1980*, p. 1231.
- [6] H. A. Lipsitt, *Mat. Res. Soc. Symp. Proc.* **1985**, 39, 351.
- [7] Y.-W. Kim, *JOM*, **1989**, 41, 24.
- [8] N. S. Choudhury, H. C. Graham, J. W. Hinze, in: *Properties of High Temperature Alloys (Z. A. Foroulis, F. S. Petit, eds.)*, The Electrochem. Soc., 1976, p. 668.
- [9] N. Zheng, H. Nickel, W. J. Quadackers, *Oxid. Met.*
- [10] S. N. Basu, J. W. Halloran, *Oxid. Met.* **1987**, 27.
- [11] W. J. Quadackers, A. Elschner, W. Speier, H. Nickel, *Appl. Surface Sci.* **1991**, 52, 271.
- [12] U. Figge, A. Elschner, N. Zheng, H. Schuster, W. J. Quadackers, *Fresenius J. Anal. Chem.* **1993**, 346, 75.
- [13] A. Gil, H. Hoven, E. Wallura, W. J. Quadackers, *Corr. Sci.* **1993**, 34, 615.



- [14] G. H. Meier, F. S. Pettit, *High Temperature Intermetallics, London, 30 April–1 May 1991*, The Royal Society, p. 66.
- [15] W. J. Quadakkers, A. Elschner, N. Zheng, H. Nickel, *12th International Corr. Congress Vol. 5B, 19–24 September, 1993, Houston, USA, NACE*, p. 3842.
- [16] G. H. Meier, F. S. Pettit, S. Hu, *J. Physique* **1993**, IV, 395.
- [17] P. Kofstad, *High Temperature Corrosion*, Elsevier, London, 1988, p. 323.
- [18] U. Figge, W. J. Quadakkers, H. Schuster, F. Schubert, in: *Proceedings EUROCORR '92' Espoo, Finland, 31 May–4 June 1992, Vol. 1*, p. 591.
- [19] K. Przybylski, A. J. Garratt-Reed, B. A. Pint, E. P. Katz, G. J. Yurek, *J. Electrochem. Soc.* **1987**, 134, 3207.
- [20] B. A. Pint, J. R. Martin, L. W. Hobbs, *Oxid. Met.*, **1993**, 39, 167.
- [21] R. A. Versaci, D. Clemens, R. Hussey, W. J. Quadakkers, *Solid State Ionics* **1993**, 59, 235.

*Received December 2, 1994. Revision April 10, 1995.*